

# A New Kinetic Lattice Monte Carlo Modeling Framework for the Source-Drain Selective Epitaxial Growth Process

Renyu Chen\*, Woosung Choi

Device Laboratory  
Samsung Semiconductor Inc.  
San Jose, CA, USA  
renyu.chen@ssi.samsung.com; renyu@uw.edu

Alexander Schmidt, Keun-Ho Lee, Youngkwan Park

Semiconductor R&D center  
Samsung Electronics  
Hwasung-si, Gyeonggi-do, Korea

**Abstract**—We have developed a new kinetic lattice Monte Carlo modeling framework for Si/Ge selective epitaxial growth based on neighbor binding interactions within the third-nearest-neighbor range of the diamond lattice. We find that first- and second-nearest-neighbor interactions contribute significantly to the faceting between {100} and {111}, while the third-nearest-neighbor interaction is the cause of {311} facet formation. The second-nearest-neighbor interaction also facilitates lateral growth and island formation within a plane. The simulated growth kinetics and shapes are in good agreement with experimental data.

**Keywords**—selective epitaxial growth; kinetic lattice Monte Carlo; source-drain engineering

## I. INTRODUCTION

Source-drain (SD) engineering to achieve optimum shape and doping profile is a key topic in TCAD design. A common source-drain fabrication method is epitaxial growth. To better control the shape and doping profile of the SD region, it is crucial to understand the underlying physics of the epitaxial growth processes. There are many experimental data regarding the growth kinetics during selective epitaxy [1]-[4]. A common phenomenon observed is faceting, which is due to the different growth rates of surface orientations. The fastest growing plane will disappear in favor of slower growing planes [1]. However, the quantitative growth and faceting kinetics vary greatly with process conditions such as gas component, flow rate, pressure, and temperature.

In the past, there are a few research activities on the atomistic modeling of epitaxial growth processes [5]-[7]. A recent paper assumes several orientation-dependent deposition rates to reproduce the faceting behavior observed in experiments [7]. This model is simple and efficient with the surface orientations determined by some heuristic rules. We have developed a kinetic lattice Monte Carlo (KLMC) modeling framework for epitaxial growth based on the physical atomic bonding interactions, without explicitly assigning specific surface orientations. We first describe the most general framework where all critical processes, including adsorption, desorption, and surface diffusion can be considered (Fig. 1). We then show a simplified

framework where only adsorption is considered with rate depending on local neighbor interactions. As selective epitaxial growth is very sensitive to process conditions, we only calibrate the model parameters with selected experiments in literature. In principle, such model parameters can be directly related to the actual process conditions; but this requires systematic experimental studies on the growth kinetics for various process conditions and is out of the scope of this paper.

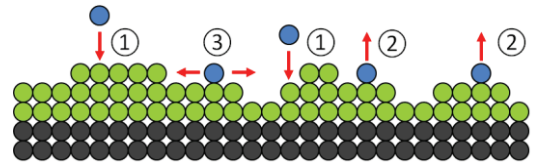


Fig. 1. Schematic of critical processes within the modeling framework: adsorption (1), desorption (2), and surface diffusion (3).

## II. GENERAL MODELING FRAMEWORK

In the general modeling framework, adsorption, desorption, and surface diffusion are considered in parallel. For adsorption, we assume a uniform rate on all surfaces with an Arrhenius form:

$$v_{\text{ads}} = v_{\text{ads}}^0 \exp\left(-\frac{E_{\text{ads}}}{kT}\right) \quad (1)$$

where  $v_{\text{ads}}^0$  and  $E_{\text{ads}}$  are the prefactor and activation energy of adsorption process, which are related to the decomposition of gas sources in the vicinity of the surface. To account for the faceting phenomenon, we assume that the desorption process is anisotropic, which depends on the total binding energy of the site

$$v_{\text{dsp}} = v_{\text{dsp}}^0 \exp\left(\frac{|E_b|}{kT}\right) \quad (2)$$

where  $E_b$  is the summation of all neighbor binding energies up to third-nearest-neighbors (3NN).

Surface diffusion events have rates calculated as

$$v_{\text{dif}} = v_{\text{dif}}^0 \exp\left(-\frac{E_{\text{m0}} + \Delta E_{\text{m}}}{kT}\right) \quad (3)$$

where  $E_{m0}$  is the unbiased diffusion barrier. The real barrier is scaled according to the energy of initial and final state of the transition [8],

$$\Delta E_m = (\Delta E_{fi} - \Delta E_{in})/2 \quad (4)$$

where  $\Delta E_{fi}$  and  $\Delta E_{in}$  are energy changes of the final and initial state due to binding interactions. This implies that atoms tend to diffuse to sites with lower energy (larger binding) due to the smaller barrier (e.g. from in to fi in Fig. 2).

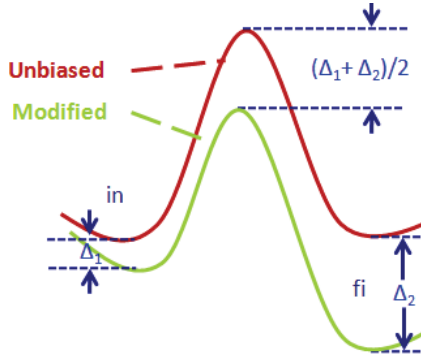


Fig. 2. Schematic for the change of migration barriers due to binding interactions of initial and final state.

The anisotropic desorption rate in (2) explains the faster growth rate of  $\{100\}$  compared to  $\{111\}$ . Let  $n_i$  be the number of  $i$ -th nearest neighbors, then an ad-atom on  $\{100\}$  surface has  $n_1 = 2$  and  $n_2 = 4$ ; an ad-atom on  $\{111\}$  surface has  $n_1 = 1$  and  $n_2 = 3$  (Ignore third-nearest-neighbor binding for now). Due to the smaller number of  $n_1$  and  $n_2$ , the ad-atoms on  $\{111\}$  surface have a smaller binding, and thus a larger desorption rate, causing the effective  $\{111\}$  growth rate to be smaller than that of the  $\{100\}$ . Eventually, all  $\{100\}$  surfaces will disappear in favor of  $\{111\}$  surfaces.

The second-nearest-neighbor (2NN) binding interactions can also account for the terrace formation during growth [1][7]. Fig. 3 shows a new layer on  $\{100\}$  and  $\{111\}$  surfaces, with the numbers in the circle being  $n_2$ . Due to the 2NN binding, surface atoms with more neighbors on the plane have lower desorption rates. This can enhance nucleation on the surface, a key step for intra-layer growth. Surface diffusion also facilitates the terrace formation, as single ad-atoms tend to migrate to the kinks and edges with larger  $n_2$ .

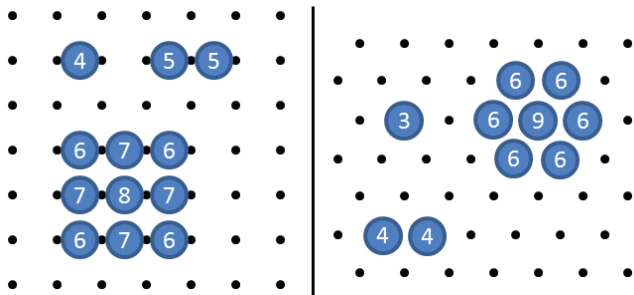


Fig. 3. Surface conditions for  $\{100\}$  (left) and  $\{111\}$  (right) surfaces. The small black dots are atoms in the underlying surface plane. The big blue

circles denote atoms on the additional surface layer, with numbers denoting the number of second-nearest-neighbors ( $n_2$ ).

The general modeling framework captures the physics of epitaxial growth by considering three types of processes. It can also simulate the etching process where desorption exceeds adsorption. However, there are several limitations. First is the relatively low efficiency. Slow growth planes such as  $\{111\}$  have high desorption rates, which implies that a large portion of CPU time is used to sample desorption events. This slows down the simulation significantly and poses challenges to large-scale and long-time growth simulations. Second, it is also very challenging to correctly simulate diffusion along rough surfaces and across different surface planes.

### III. SIMPLIFIED MODELING FRAMEWORK

For applications where deposition is the dominant process, we have further simplified the framework by only considering the adsorption process, with rates determined by local neighbor interactions. Such treatment has been adopted earlier in [6]. We considered binding interactions up to 3NN. The adsorption rate is calculated as

$$v_{\text{ads}} = v_{\text{ads}}^0 v_c(n_1) \exp\left(-\frac{E_{\text{ads}}^0 - |E_b|}{kT}\right) \quad (5)$$

where  $v_{\text{ads}}^0$  and  $E_{\text{ads}}^0$  are the base-line prefactor and activation energy for adsorption, which are related to the dissociation of gas species.  $v_c(n_1)$  is the additional correction factor for sites with different values of  $n_1$ . This takes into account any entropy changes due to the presence of first-nearest-neighbors. For a simple model, the  $v_c$ 's are the same for all  $n_1$ .  $E_b$  is the total binding energy related to the atom if it is deposited on the site. The binding of the deposited atom to the neighboring atoms reduces the total activation energy, and thus enhances adsorption. This is in the same spirit as in (4), except for the  $1/2$  factor. The total binding energy is calculated as

$$E_b = E_b^{1NN}(n_1) + n_2 E_b^{2NN} + n_3 E_b^{3NN} \quad (6)$$

where  $n_i$  is the number of  $i$ -th nearest neighbors.  $E_b^{2NN}$  and  $E_b^{3NN}$  are binding energies of each 2NN and 3NN pair. Contributions of 2NN and 3NN binding are added linearly. For 1NN interactions, due to the possible distortion of bonds, a non-linear interaction model is used, which tabulates the binding energies for different  $n_1$  values.

## IV. RESULTS AND DISCUSSIONS

### A. Planar Growth Simulations

For planar growth simulations, the simple framework where only adsorption is considered gives similar results to that of the general framework, but is around ten times more efficient. Here only results obtained by using the simple framework are shown. We calibrated the parameters using the observed growth data in [2] [3]. The parameter values are listed in Table I. The energy values represent the "effective" binding lumping desorption and diffusion contributions. They may not be directly comparable to the real Si-Si bond

energy. Also, the large surface constructions can also change the binding interactions significantly.

The simulated growth rates as functions of temperature are shown in Fig. 4. The activation for  $\{100\}$  surface is extracted to be 1.7 eV, consistent with [2] (although therein the authors incorrectly extracted the value of 2.05 eV). The ratio of  $\{311\}$  and  $\{111\}$  growth rates to that of  $\{100\}$  at 700 °C is calculated to be 0.59 and 0.34 respectively, which agrees with the experimental values of 0.63 and 0.30 in [3]. The activation energies of  $\{111\}$  and  $\{311\}$  are very close to (though slightly higher than) that of  $\{100\}$ .

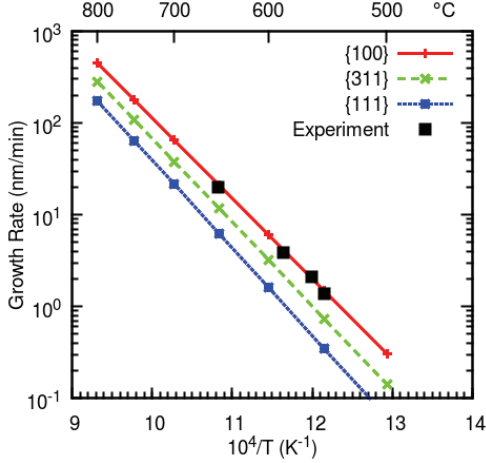


Fig. 4. Calculated growth rates under different temperatures in comparison with experimental data [2].

Table I. Parameters used for growth simulation within the simple framework.

Parameter	$n_1 = 1$	$n_1 = 2$	$n_1 = 3$
$v_{\text{ads}}^0$ (/s)	$5.6 \times 10^9$		
$v_c$	1.0	1.0	1.0
$E_{\text{ads}}^0$ (eV)	3.7		
$E_b^{1NN}$ (eV)	0.40	0.50	0.75
$E_b^{2NN}$ (eV)	0.15		
$E_b^{3NN}$ (eV)	0.12		

Using the same set of parameters, we investigated the growth for individual planar surfaces at 800 °C. A  $20 \times 20$  nm<sup>2</sup> square plane is used as initial substrate with periodic boundaries on the two sides. The intermediate growth structures are shown in Fig. 5, with common  $\langle 110 \rangle$  edges within the plane denoted by red dashed lines. It can be seen that the second-nearest-neighbor interactions play an important role for the nucleation of adatoms on a newly-grown surface layer. Sites with more  $n_2$  (e.g. those near kinks and edges) are more favorable for adsorption. This effectively takes into account the diffusion of atoms towards these low energy sites, without explicitly simulating diffusion. Rectangular terraces for the  $\{100\}$  surfaces are formed, consistent with [1]. On  $\{111\}$  surfaces, irregular terraces with ledges along the three equivalent  $\langle 110 \rangle$  directions co-exist with single adatoms. On  $\{311\}$  surfaces, atoms tend to aggregate along the  $\langle 110 \rangle$  channel as shown in

Fig. 5(c). The dimer-like structures along the  $[33\bar{2}]$  direction are first nearest neighbor pairs.

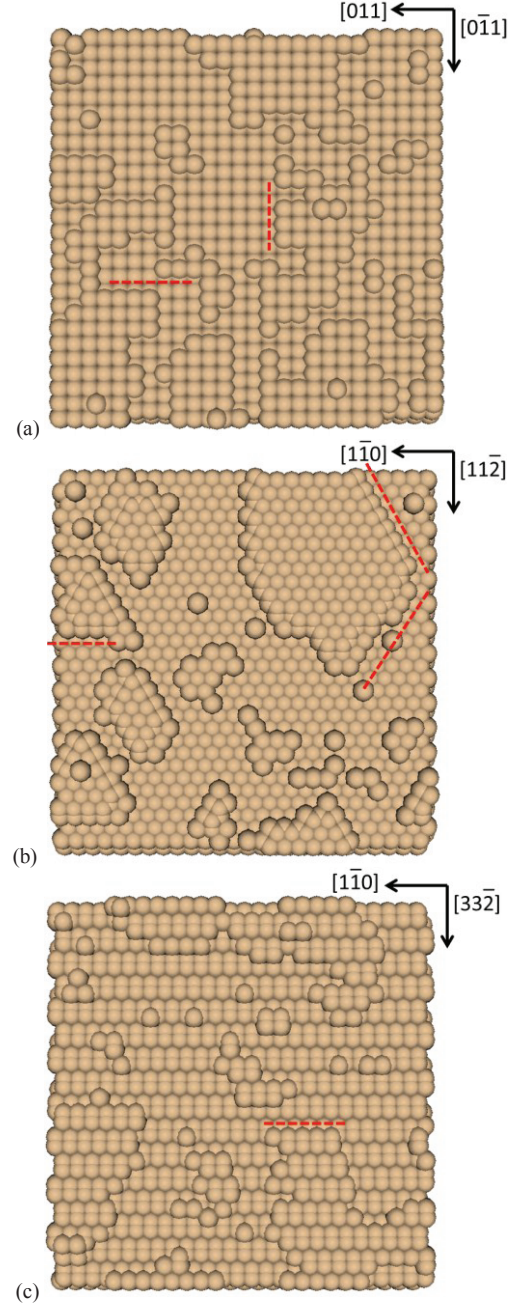


Fig. 5. Simulation of growth on (a)  $\{100\}$ , (b)  $\{111\}$ , and (c)  $\{311\}$  planar surfaces.

### B. Faceting Simulations

We carried out quasi-2D faceting simulations on a  $\{100\}$  surface with non-periodic boundary condition on  $[110]$  at 600 °C (Fig. 6). Periodic boundary condition is applied on  $[\bar{1}10]$ . Growth fronts at several time stages are shown. We can see the initial development of  $\{311\}$  planes, and then the catching up of  $\{111\}$  planes at later stages. This is consistent with experimental observations in [4].

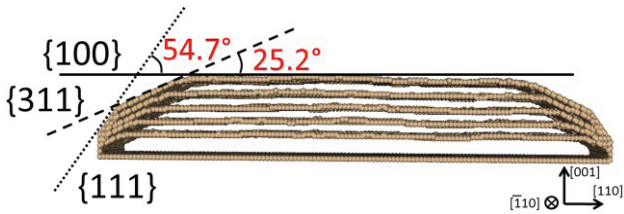


Fig. 6. Quasi-2D simulation of growth bounded by “hard walls” along  $[110]$ . Growth fronts at several stages are shown. The length along  $[110]$  is 50 nm.

To understand this behavior, the bonding environment of a new ad-atom on a clean surface is shown in Table II. With the parameter values in Table I, it can be seen that adatoms deposit much slower on  $\{111\}$  than on  $\{100\}$  due to the lower binding. For  $\{311\}$ , initially the co-existence of sites with  $n_1$  being 1 and 2 makes its growth faster than  $\{111\}$ . Due to a smaller  $n_3$  of  $\{311\}$  compared to  $\{100\}$ ,  $\{311\}$  grows slower than  $\{100\}$ . This is in the same spirit as in [7] where atoms with fewer  $n_3$  are assigned a lower rate of adsorption. Because  $\{311\}$  forms a smaller angle to  $\{100\}$  as shown in Fig. 6,  $\{311\}$  appears first. The  $\{311\}$  planes will finally give way to  $\{111\}$  planes due to the larger growth rate of  $\{311\}$  compared to  $\{111\}$ .

Table II. Number of neighbors of an ad-atom on a clean surface.

Surface Plane	$n_1$	$n_2$	$n_3$
$\{100\}$	2	4	6
$\{111\}$	1	3	6
$\{311\}$	1; 2	5	4

We also performed a growth simulation inside a trench structure similar to [9]. Due to the lack of information on the actual dimension and process conditions, we use a geometry that is in proportion to the TEM image and a typical process temperature of 600 °C. Parameters are slightly changed from Table I to give a closer prediction. The growth fronts at different stages are shown in Fig. 7. The oxide region only acts as a boundary material and thus does not interact with the grown atoms. The simulated intermediate and final shapes agree well with the TEM image in the inset of Fig. 7.

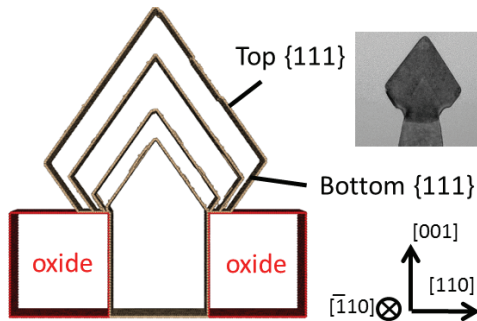


Fig. 7. Quasi-2D simulation of growth in a trench structure. Inset shows TEM image from [9]. The trench width in the simulation is 20 nm.

We also performed a 3D simulation using the general framework where diffusion and desorption are also considered. The simulated final structure is shown in Fig. 8. Due to the non-periodic condition along  $[110]$ , more  $\{111\}$

facets appear, resulting in a pyramid-shaped structure. The overall shape is consistent with the TEM image in Fig. 7.

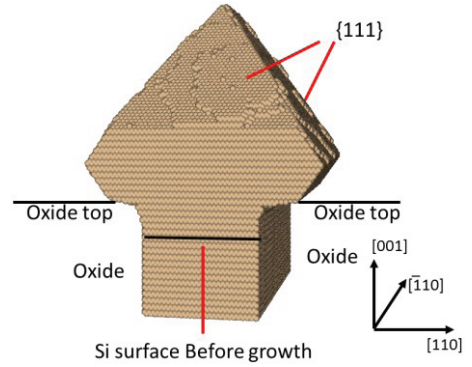


Fig. 8. 3D simulation of growth in a trench structure within the full simulation framework, where adsorption, diffusion, and desorption are considered.

## V. CONCLUSION

We have developed a new KLMC simulation framework for source-drain epitaxial growth process that can quantitatively simulate the growth kinetics and faceting behavior. Simulation results are in good agreement with various experimental data which indicates the great potential of the simulator in the application for optimization of real source-drain fabrication processes.

## ACKNOWLEDGMENT

The authors gratefully acknowledge Dr. Hong-Hyun Park for his significant contributions to code development and Professor Scott Dunham and Haoyu Lai for many fruitful discussions.

## REFERENCES

- [1] H. Hirayama, M. Hiroi, and T. Ide, “ $\{311\}$  facets of selectively grown epitaxial Si layers on  $\text{SiO}_2$ -patterned Si(100) surfaces,” *Phys. Rev. B*, vol. 48, pp. 17331-17337, 1993.
- [2] H.-C. Tseng, C. Y. Chang, F. M. Pan, J. R. Chen, and L. J. Chen, “Effects of isolation materials on facet formation for silicon selective epitaxial growth,” *Appl. Phys. Lett.*, vol. 71, pp. 2328-2330, 1997.
- [3] L. Vescan, K. Grimm, and C. Dieker, “Facet investigation in selective epitaxial growth of Si and SiGe on (001) Si for optoelectronic devices,” *J. Vac. Sci. Technol. B*, vol. 16, pp. 1549-1554, 1998.
- [4] T. Aoyama, T. Ikarashi, K. Miyanaga, and T. Tatsumi, “Facet formation mechanism of silicon selective epitaxial layer by Si ultrahigh vacuum chemical vapor deposition,” *J. Cryst. Growth*, vol. 16, p. 349, 1994.
- [5] A. Ishitani, T. Takada, and Y. Ohshita, “Charge transfer adsorption in silicon vaporphase epitaxial growth,” *J. Appl. Phys.*, vol. 63, p. 390, 1987.
- [6] T. Kawamura, “Monte Carlo simulation of thin film growth on Si surfaces,” *Prog. Surf. Sci.*, vol. 44, pp. 67-99, 1993.
- [7] I. Martin-Bragado and V. Moroz, “Modeling of  $\{311\}$  facets using a lattice kinetic Monte Carlo three-dimensional model for selective epitaxial growth of silicon,” *Appl. Phys. Lett.*, vol. 98, p. 153111, 2011.
- [8] M. Bunea and S. Dunham, “Monte Carlo study of vacancy-mediated impurity diffusion in silicon,” *Phys. Rev. B*, vol. 61, p. R2397, 2000.
- [9] C. Auth, et al., “A 22nm high performance and low-power CMOS technology featuring fully-depleted tri-gate transistors, self-aligned contacts and high density MIM capacitors,” 2012 Symposium on VLSI Technology, pp.131-132, Hawaii, June 2012.